Towards the Fabrication of the Top-Contact Electrode in Molecular Junctions by Photoreduction of a Metal Precursor

Santiago Martín,[a,b,c] Gorka Pera,[a,d] Luz M. Ballesteros,[a, d] Adam J. Hope,[e] Santiago Marqués-González,[e] Paul J. Low,[e] Francesc Pérez-Murano,[f] Richard J. Nichols,[g] and Pilar Cea [a, c,d*]

[a] Departamento de Química Física, Facultad de Ciencias, Universidad de Zaragoza, 50009, Spain.

[b] Instituto de Ciencias de Materiales de Aragón (ICMA), Universidad de Zaragoza-CSIC, 50009 Zaragoza, Spain.

[c)] Laboratorio de Microscopías Avanzadas (LMA), Universidad de Zaragoza, 50018 Zaragoza, Spain.

[d)] Instituto de Nanociencia de Aragón (INA), edificio i+d Campus Rio Ebro, Universidad de Zaragoza, C/Mariano Esquillor, s/n, 50018 Zaragoza (Spain)

[e)] Department of Chemistry, University of Durham, Durham DH1 3LE, United Kingdom.

[f)] Instituto de Microelectrónica de Barcelona (IMB-CNM, CSIC), Campus UAB, 08193 Bellaterra, Spain

[g)] Department of Chemistry, University of Liverpool, Crown Street, Liverpool, L69 7ZD, United Kingdom.

*Corresponding author: pilarcea@unizar.es

Abstract

In this contribution a method is described to fabricate the top-contact electrode in metal|molecule|metal devices by photoreduction of a metal precursor. In particular, $AuCl_4^-$ anions have been incorporated onto a Langmuir-Blodgett (LB) film containing an ionisable oligo(phenylene-ethynylene) (OPE) derivative. Conditions appropriate for deposition of these monolayers onto solid supports have been established and subsequent photoreduction lead to the formation of metallic gold nano-islands distributed on the surface of the film. Electrical properties of these devices were determined by recording *I-V* curves with a conductive-AFM using the Peak Force Tunneling AFM (PF-TUNA™) mode. The obtained results rule out the formation of short-circuits showing that photoreduction of a metal precursor incorporated onto monomolecular films is an effective method for the fabrication of molecular junctions.

Key words: Langmuir-Blodgett films, metal-molecule-metal junctions, photoreduction, top-contact electrode.

Introduction

The quest towards further miniaturization of electronic devices has led to increasing interest in organic molecules as functional elements within a hybrid solid-state/ molecular technology.[1-3] Significant progress in the synthesis of new molecules with inherent electronic function and compatibility with device-like architectures has been made in the last decade[4-12] but many scientific and technological challenges remain to be addressed before molecular electronics can be considered a viable technology and reach the market. One of these challenges is the reliable deposition of the second ("top") electrode in two terminal sandwich-based metal|organic|metal devices. Several recent papers[13-16] have critically reviewed the techniques available for the deposition of the top-contact electrode, summarizing the approach used and highlighting the advantages and serious limitations of these methods. Perhaps the most significant problems in the deposition of the second electrode are those related to damage of the functional molecules during the metallization of a monolayer or penetration of the second metal through the organic films, which results in a short circuit, rendering the device unusable.

In contrast to thermal processing methods, such as metal evaporation and sputtering, photochemical based approaches are compatible with both solid state and molecular materials. Indeed, photolithography is one of the most important processing techniques used in conventional (solid state) electronics fabrication. Photoreduction of metal precursors to produce metal nanoparticles (NPs) or clusters incorporated in thin films has been reported in the literature for different applications,[17-23] and the compatibility of these methods with molecular substructures has inspired the work described here. In this work, a metal precursor ($AuCl_4^-$) is incorporated onto a Langmuir-Blodgett (LB) film during the fabrication process, with subsequent photoreduction leading to the formation of metallic gold nano-islands (GNIs) on top of the intact molecular film. The metal|molecule|GNI systems are free of metallic inter-penetration and short circuits providing a route to nascent device structures. Although the concept of photoreducing a metal precursor on top of a molecular film could be applied to monolayers prepared by other approaches (e.g. self-assembled films) we have chosen the LB technique as the metal precursor can be easily incorporated on top of the LB film during the transfer of

Código de campo cambiado

Código de campo cambiado

Código de campo cambiado

Código de campo cambiado

the films from the air-liquid interface without any additional step in the fabrication process.[24-25] In addition, the LB method has broad applicability to a wide range of molecular systems since it can be used to form both chemisorbed and physisorbed films, which significantly broadens the range of molecular systems and surfaces that can be employed in a junction.[26] This flexibility of molecule and surface is important as systematic studies of different organic-metal contacts are crucial to determine the role that the interface plays in the performance of molecular devices.[27-31] Directionally oriented films can also be prepared by the LB technique, which in turn offers a significant degree of control over the final architecture and functionality of the devices, and is especially important considering that molecules incorporated into a metal|molecule|metal devices need to be bi-functional in order to permit strong binding to both metal interfaces.[32-33] Although electrochemical methods have been successful used for the fabrication of metal films on-top of self-assembled monolayers,[34-37] these methods clearly require polarisation of the substrate within an electrochemical cell which is likely to be unpractical for many device applications. By contrast, the photolytic method is "contact" free and requires only optical illumination over the substrate area.

Código de campo cambiado
Código de campo cambiado
Código de campo cambiado
Código de campo cambiado
Código de campo cambiado

Results and Discussion

Oligo(phenylene) ethynylene based structures have long been used as prototype molecular wires and have been shown to be robust platforms for exploration of various aspects of molecular electronic science from the development of measurement methods, length dependent conductance mechanisms and novel surface contact chemistry.[38-51] Figure 1 shows the chemical structure of the oligomeric phenylene ethynylene (OPE) derivative used in this work, henceforward abbreviated as [**1H**]Cl. It contains a highly hydrophobic group, –C≡CSiMe$_3$, which has been recently demonstrated[47, 52] as an effective surface anchoring group that provides direct electronic coupling at metal-molecule contacts, presumably through interaction between the terminal Si atom and the metal substrate. The other terminal group of this material is a hydrophilic group that facilitates the anchoring of the molecule at the water surface, providing stability to the Langmuir films. In addition, the hydrophilicity difference between the two terminal

Código de campo cambiado
Código de campo cambiado
Código de campo cambiado

groups is expected to permit the fabrication of directionally oriented films in which the $–C{\equiv}CSiMe_3$ group will be deposited onto the bottom gold electrode and the hydrophilic NH_3^+ group is then away from the surface. The Cl^- anion associated with the $–NH_3^+$ terminus is readily exchanged for other ions, such as the $AuCl_4^-$ anion, introduced into the aqueous subphase.

Figure 1 shows representative surface pressure vs. area per molecule (π-*A*) isotherms of **[1H**]Cl on a pure water subphase and a $2{\cdot}10^{-5}$ M $HAuCl_4$ aqueous subphase. The π-*A* isotherm obtained for a pure water subphase features a lift-off at ca. 0.60 $nm^2{\cdot}molecule^{-1}$. The monolayer prepared onto a $HAuCl_4$ aqueous subphase, comprised of [**1H**]$AuCl_4$ after anion exchange, shows the lift-off at a slightly higher area, ca. 0.65 $nm^2{\cdot}molecule^{-1}$. Upon compression isotherms from films of both [**1H**]Cl and [**1H**]$AuCl_4$ show a monotonic increase of the surface pressure until the collapse is reached at surface pressures around 45 $mN{\cdot}m^{-1}$ in both cases. The higher areas per molecule obtained at the same surface pressure for the isotherm recorded for [**1H**]$AuCl_4$ derived films are indicative of the incorporation of the relatively large $AuCl_4^-$ anions into the monolayer.[24]

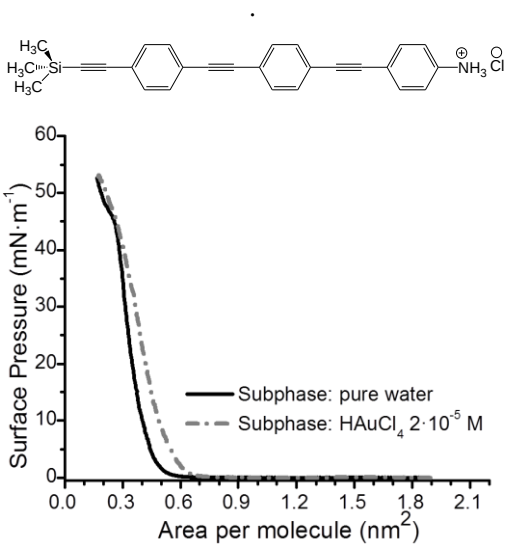

Figure 1. Chemical structure and surface pressure vs. area per molecule isotherms of [**1H**]Cl onto a pure water subphase and a $2{\cdot}10^{-5}$ M $HAuCl_4$ aqueous subphase.

Langmuir monolayers of [**1H**]$AuCl_4$ were transferred onto solid substrates - initially outside of the aqueous $HAuCl_4$ subphase - by the vertical dipping method at a surface pressure of 20 $mN{\cdot}m^{-1}$ to form one-layer LB films. The transfer ratio (defined as the decrease in monolayer area during the deposition divided by the area of the substrate) calculated using the trough software was 1. Under these transfer conditions (substrates initially outside of the subphase) the trimethylsilyl group is directly attached to the substrate[47] with XPS experiments confirming chemisorption of this group onto gold substrates (see supporting information).[53-54]

Figure 2 shows the UV-vis spectrum of a pristine one-layer LB film of [**1H**]$AuCl_4$ transferred onto a quartz substrate. This spectrum features a band at 345 nm, which is likely to result from unresolved π-π^* transitions associated with the OPE backbone[55] which appears at the same wavelength as the analogous transitions of [**1H**]Cl in solution (see supporting information). Irradiation of the [**1H**]$AuCl_4$ LB film with UV light (254 nm) results in a reduction in the intensity and blue shift of the absorption envelope at 345 nm. These changes in the spectrum are accompanied by the appearance of a small broad peak at ca. 550 nm, attributable to surface plasmon resonance of gold nanoparticles.[56] Further irradiation of the film yields an increase in the gold plasmon band and a further decrease and blue shift of the OPE main band. After 90 minutes of irradiation the maximum absorption band is shifted to λ_{max} = 328 nm. Further irradiation times did not produce any significant increase in the gold plasmon band. A Au|$Me_3SiC{\equiv}C$-OPE-NH_3Cl LB film (fabricated from a Langmuir film onto a pure water subphase) was also subjected to irradiation under the same conditions as the Au|$Me_3SiC{\equiv}C$-OPE-NH_3AuCl_4 film, with no change in the UV spectral profile (see supporting information). This suggests photodamage to the OPE backbone is unlikely the cause of the change in spectroscopic profile observed during photolysis of Au|$Me_3SiC{\equiv}C$-OPE-NH_3AuCl_4 LB films. Rather, the different chemical environment of the organic moiety together with a possible change in the tilt angle of the molecules or the interaction of the molecules with the generated gold nano-islands are more plausible reasons for the blue-shift observed for the main peak.

Código de campo cambiado

Código de campo cambiado

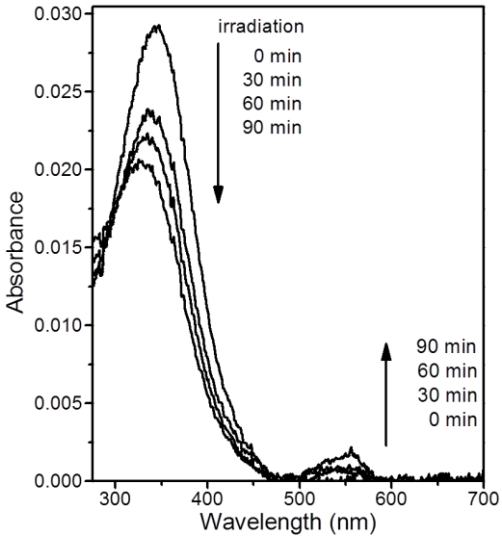

Figure 2. UV-vis spectra of a pristine [**1H**]$AuCl_4$ one-layer LB film and the same film after irradiation with UV light at 254 nm for the indicated periods of time.

The observation of a plasmon band is consistent with the formation of gold nano-islands (GNIs) on top of the LB film after irradiation. Formation of Au(0) has also been demonstrated by XPS. Figure 3 shows the XPS spectra of pristine and irradiated [**1H**]$AuCl_4$ LB films on a glass substrate. The Au4f region for the film after irradiation shows two peaks at 84.1 and 87.8 eV, whilst the XPS-spectrum of the pristine film exhibits two intense peaks at 84.7 and 88.4 eV. This shift to lower binding energies upon irradiation is consistent with the reduction of the gold precursor to Au(0).[57-60]

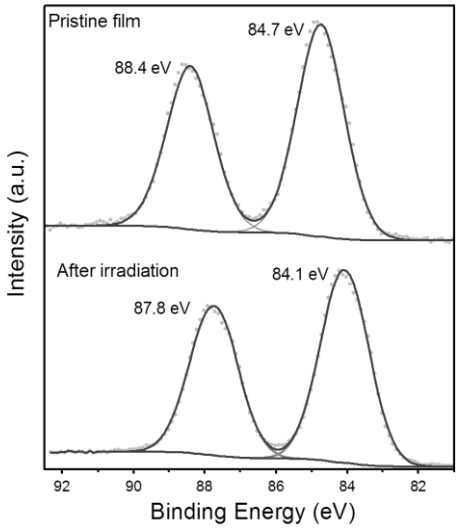

Figure 3. XPS spectra of Au4f photoelectrons of pristine and 90 minutes irradiated (254 nm) [**1H**]$AuCl_4$ LB films.

The photoreduction process of is considered to proceed through the mechanism described by Kurihara et. al.[61] and Yonezawa et al.[62]:

(1)

(2)

(3)

– (4)

In addition, gold atoms tend to diffuse on the surface and aggregate to form gold nano-islands $(Au^0)_n$.

However, neither UV-vis spectroscopy nor XPS provide any information about the distribution of the GNIs on the surface of the film. To investigate this issue, scanning electron microscopy (SEM) images of LB films after irradiation have been obtained (see a representative image in Figure 4). SEM images indicate that the LB film

is decorated with gold islands (GNIGNIs) with a close to circular appearance, most of these GNIs having diameters in the 5-20 nm range.

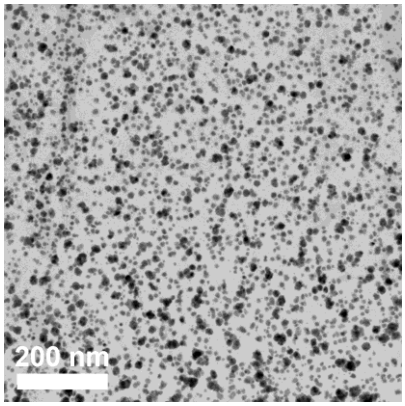

Figure 4. SEM image of a one layer [**1H**]$AuCl_4$ LB film deposited onto a glass substrate film after 90 minutes of irradiation with UV light at 254 nm.

The formation of GNIs on the LB monolayer was also studied by atomic force microscopy (AFM). Figure 5 shows an AFM image of a mica|$Me_3SiC{\equiv}C$-OPE-NH_3AuCl_4 monolayer before and after irradiation for 90 minutes. The pristine film shows a homogeneous surface with a low root mean square (RMS) roughness of 0.076 nm and a surface practically free of three dimensional defects or holes. In contrast, after irradiation the film shows a significant increase in the roughness (RMS=0.393 nm) together with the appearance of round and bright spots distributed all over the film revealing the presence of GNIs. A section analysis of the AFM images has revealed that the average height of these GNIs is 0.7 nm with a few GNIs (ca. 1% of the total film area according to the bearing analysis) exhibiting higher heights (up to a maximum of 2.5 nm). This means that the gold nano-islands have a high aspects ratio and can be described as having a pancake type morphology.

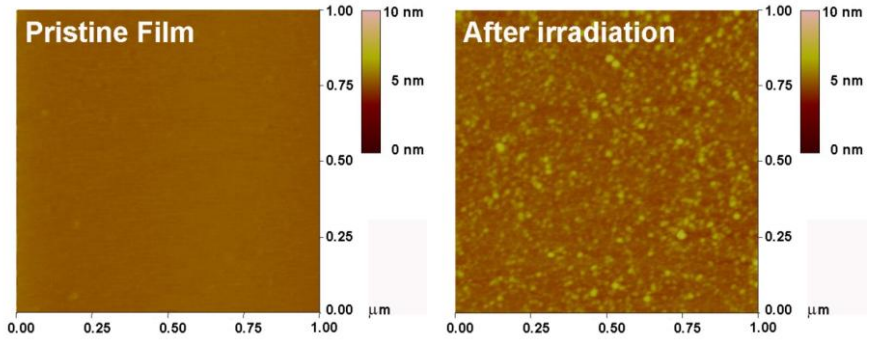

Figure 5. AFM images of a one layer [**1H**]$AuCl_4$ LB film deposited onto a mica substrate before and after irradiation with 254 nm light for 90 minutes.

A frequent problem in the fabrication of the top contact electrode is the formation of short-circuits due to a metallic contact between the bottom and top-contact electrodes.[63-65] Therefore, it is important to verify whether the metal contacting strategy proposed in this paper also leads to short-circuits or whether on the contrary it is an effective technique for avoiding such a problem. To probe the electrical properties of the metal|organic monolayer|GNIs sandwich structures fabricated as described above, *I-V* curves were recorded with a conductive-AFM (Bruker ICON) using the Peak Force Tunneling AFM (PF-TUNA™) mode and a PF-TUNA™ cantilever from Bruker (coated with Pt/Ir 20 nm, ca. 25 nm radius, 0.4 $N \cdot m^{-1}$ spring constant and 70 kHz resonance frequency).[66-69] The PF-TUNA™ operation mode for the AFM was chosen in order to avoid lateral forces during the imaging that would have damaged the tip coating and sample surface, while at the same time allowing the use of cantilevers with a low spring constant. Thus, this is a method for the conductivity mapping of soft or fragile samples and as such it has been chosen for conductivity probing of our metal|organic monolayer|GNIs, rather than using STM or conducting AFM in conventional contact mode. The Peak Force Tunneling AFM used here combines "tapping" mode AFM with a conducting AFM tip and low-noise current amplifier to probe current flow through the metal|organic monolayer|GNI junctions. A compromise has to be made in selecting the peak force which is applied during the measurement. Too much force will result in unacceptably large deformation of the monolayer underlying the GNIs, while too little force will result in inadequate electrical probing. Therefore, before recording the *I-V* curves control experiments have been made to

determine the most suitable set-point force. This entailed monitoring the deformation or damage to the monolayer as a function of tip loading force (set-point force) and these data are presented in the supporting information. These measurements showed that a set-point force of around 34 nN is required to make a reasonable contact between the tip and the GNI while avoiding damage or excessive deformation of the organic layer during the determination of the electrical properties. Using this force set-point *I-V* curves were then recorded with the AFM probe placed on top of GNIs and a bias between the substrate and the tip was applied. *I-V* characteristics were recorded by sweeping the tip voltage (±1.1 V) with the LB-coated Au substrate held at ground. To ensure reproducibility and reliability of the results, the *I-V* curves were averaged from multiple scans. Figure 6 shows an averaged *I-V* curve for the metal⏐organic monolayer⏐GNIs sandwich structures recorded using a set-point force of 34 nN. These curves show a shape commonly observed for metal-molecule-metal junctions, with a linear section only at relatively low bias voltages and increasing curve gradients at higher bias. Most importantly, only curves like this were observed and no low resistance traces characteristic of metallic short circuits were obtained over a wide range of set-point forces. These observations rule out the presence of short-circuits. These results confirm that robust and reliable top-contacts have been prepared without damaging the organic layer or altering/contaminating the interfaces avoiding electronic or structural rearrangements. Therefore, this shows that the fabrication of the top-contact electrode by photoreduction of a metal precursor is an alternative to other traditional methods.

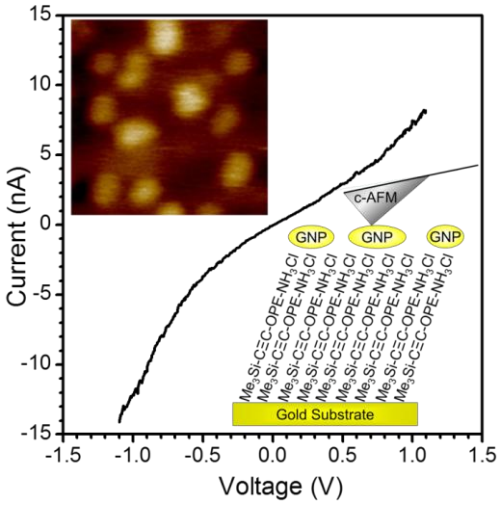

Figure 6. Averaged *I-V* curve over 350 curves obtained by positioning the c-AFM tip on top of GNIs generated by irradiation of an Au|$Me_3SiC{\equiv}C$-OPE-NH_3AuCl_4 monomolecular LB film. The set-point force used was 34 nN. The inset top image shows a representative example of a 200 x 200 nm^2 image where gold NPs can be clearly distinguished and was used to position the c-AFM tip onto the NPs. The inset bottom image shows a scheme of the studied metal|organic monolayer|GNIs sandwich structures.

Conclusions

In this paper photoreduction of a metal precursor ionically bound to a LB film is shown to be suitable for the fabrication of top-contact GNIs in molecular junctions. This has proved to be an efficient and reliable technique for the fabrication of a top contact of organic monolayers that minimizes the appearance of short-circuits which is a rather common problem in other traditional methods for the preparation of top contact electrodes. Moreover, this method avoids expensive deposition techniques for the top contact electrode. In addition, the photoreduction technique could be easily applicable in other type of monolayers, including self-assembled ones. Moreover, we can envision the use of other metal precursors including silver, platinum or copper ions. If needed these GNIs could be used as seeds for deposition of a thicker and contiguous metal film top contact using other methods (e.g., electroless metal deposition), leading ultimately

to a controlled preparation of molecular electronic junctions with a significant inhibition in the formation of short-circuits.

Experimental Section

Film fabrication. 4-((4-((4-((trimethylsilyl)ethynyl)phenyl)ethynyl) phenyl)ethynyl) benzenaminium chloride ([**1H**]Cl) was prepared as described in the supporting information. A Nima Teflon trough with dimensions 720 × 100 mm^2 housed in a constant temperature (20±1 ºC) clean room was used to prepare the films. The surface pressure (π) of the monolayers was measured by using a Wilhelmy paper plate pressure sensor. Ultrapure Millipore Milli-Q® water (resistivity 18.2 MΩ·cm) was used as sub-phase. The spreading solutions $2.5 \cdot 10^{-5}$ M in [**1H**]Cl were prepared in chloroform (HPLC grade, 99.9 % purchased from Sigma). To construct the Langmuir films, the solution was spread using a Hamilton micro-syringe held very close to an aqueous surface, allowing the surface pressure to return to a value as close as possible to zero between each addition. The spreading solvent was allowed to completely evaporate over a period of at least 15 min before compression of the Langmuir film at a constant sweeping speed of 0.02 $nm^2 \cdot molecule^{-1} \cdot min^{-1}$.

The films were deposited at a constant surface pressure by the vertical dipping method with a dipping speed of 0.6 $cm \cdot min^{-1}$. The solid substrates used to support the LB films were quartz, mica, glass, and gold. Gold substrates were purchased from Arrandee®, Schroeer, Germany and were flame-annealed at approximately 800-1000 ºC with a Bunsen burner immediately prior to use to prepare atomically flat Au(111) terraces.[70] UV-visible spectra were acquired on a Varian Cary 50 spectrophotometer, and recorded using a normal incident angle with respect to the film plane. Atomic Force Microscopy (AFM) experiments were performed by means of a Multimode 8 AFM system from Veeco, using the tapping mode. The data were collected with a silicon cantilever provided by Bruker, with a force constant of 40 mN and operating at a resonant frequency of 300 kHz. The images were collected with a scan rate of 1 Hz, an amplitude set point lower than 1 V, and in ambient air conditions. Scanning electron microscopy (SEM) images were obtained with a JEOL JSM 6400 microscope. X-ray photoelectron spectroscopy (XPS) spectra were acquired on a Kratos AXIS ultra DLD spectrometer with a monochromatic Al Kα X-ray source (1486.6 eV) using a pass

energy of 20 eV. To provide a precise energy calibration, the XPS binding energies were referenced to the C1s peak at 284.6 eV. Electrical properties of the molecular junctions were recorded with a conductive-AFM (Bruker ICON) under humidity control, ca. 30%, with a N_2 flow using the Peak Force Tunneling AFM (PF-TUNA™) mode, and employing a PF-TUNA™ cantilever from Bruker (coated with Pt/Ir 20 nm, ca. 25 nm radius, 0.4 $N \cdot m^{-1}$ spring constant and 70 kHz resonance frequency).

Acknowledgments

S.M. F.P.-M and P.C. are grateful for financial assistance from Ministerio de Economía y Competitividad from Spain and fondos FEDER in the framework of projects CTQ2012-33198, CSIC10-4E-805, and CSD2010-00024. S.M., F.P-M and P.C. are also grateful to the European SUDOE TRAIN2 project and the Nanolito network through the MAT2011-13099-E project funded by the Ministry of Economy of Spain for supporting this collaborative work. R.J.N., P.J.L. and S.M-G. thank EPSRC for funding. G.P. gratefully acknowledges the award of a FPU fellowship from MEC and L.M.B acknowledges her grant from Banco Santander.

References

[1] D. Nilsson, S. Watcharinyaron, M. Eng, L. Li, E. Moons, L. Johanson, M. Zharnikov, A. Shaporenko, B. Albinsson, J. Martensson, *Langmuir* **2007**, *23*, 6170-6181.
[2] A. M. Rawlett, T. J. Hopson, I. Amlani, R. Zhang, J. Tresek, L. A. Nagahara, R. K. Tsui, H. Goronkin, *Nanotechnology* **2003**, *14*, 377-384.
[3] U. H. F. Bunz, *Adv. Polym. Sci.* **2005**, *177*, 1-52.
[4] V. Balzani, A. Credi, M. Venturi, *Molecular Devices and Machines: A Journey into the Nanoworld*, Wiley-VCH, Weinhein, **2003**.
[5] C. Wang, A. S. Batsanov, M. R. Bryce, S. Martin, R. J. Nichols, S. J. Higgings, V. M. Garcia-Suarez, C. J. Lambert, *J. Am. Chem. Soc.* **2009**, *131*, 15647-15654.
[6] A. K. Mahapatro, J. W. ing, T. Ren, D. B. Janes, *Nano Lett.* **2008**, *8*, 2131-2136.
[7] J. M. Tour, *Chem. Rev.* **1996**, *96*, 537-553.
[8] L. Welte, A. Calzolari, R. Di Felice, F. Zamora, J. Gomez-Herrero, *Nat. Nanotechnol.* **2010**, *5*, 110-115.

[9] S. Higgins, R. J. Nichols, S. Martin, P. Cea, H. S. J. Van der Zant, M. M. Richter, P. J. Low, *Organometallics* **2011**, *30*, 7-12.
[10] Z. L. Cheng, R. Skouta, H. Vazquez, J. R. Widawsky, S. Schneebeli, W. Chen, M. S. Hybertsen, R. Breslow, L. Venkataraman, *Nat. Nanotechnol.* **2011**, *6*, 353-357.
[11] E. Leary, M. T. González, C. van der Pol, M. R. Bryce, S. Filipone, N. Martin, G. Rubio-Bollinger, N. Agrait, *Nano Lett.* **2011**, *11*, 2236-2241.
[12] S. Battacharyya, A. Kibel, G. Kodis, P. A. Liddell, M. Gervaldo, D. Gust, S. Lindsay, *Nano Lett.* **2011**, *11*, 2709-2714.
[13] H. Haick, D. Cahen, *Prog. Surf. Sci.* **2008**, *83*, 217-261.
[14] H. B. Akkerman, B. de Boer, *J. Phys.: Condens. Matter* **2008**, *20*, 013001 (013020pp).
[15] D. Vuillaume, *C. R. Physics* **2008**, *9*, 78-94.
[16] D. Vuillaume, *Proceedings of the IEEE* **2010**, *1-12*.
[17] S. Ravaine, G. E. Fanucci, C. T. Seip, J. H. Adair, D. R. Talham, *Langmuir* **1998**, *14*, 708-713.
[18] A. Alexandrov, V. Smirnova, N. Yakimovich, N. Sapoova, L. Soustov, A. Kirsanov, N. Bityurin, *Appl. Surf. Sci.* **2005**, *248*, 4.
[19] E. Ozkaraoglu, I. Tunc, S. Suzer, *Polymer* **2009**, *50*.
[20] E. Yilmaz, S. Suzer, *Appl. Surf. Sci.* **2010**, *256*.
[21] M. Kimura, T. Hatanaka, H. Nomoto, J. Kakizawa, T. Fukawa, Y. Tatewaki, H. Shirai, *Chem. Mater.* **2010**, *22*.
[22] L. Zhong, T. Jiao, M. Liu, *Langmuir* **2008**, *24*, 11677-11683.
[23] X. Bai, L. Zheng, N. Li, B. Dong, H. Liu, *Crystal Growth & Design* **2008**, *8*, 3840-3846.
[24] S. Martín, P. Cea, C. Lafuente, F. M. Royo, M. C. López, *Surf. Sci.* **2004**, *563*, 27-40.
[25] P. Cea, S. Martín, A. Villares, D. Möbius, M. C. López, *J. Phys. Chem. B* **2006**, *110* 963-970.
[26] S. Gyepi-Garbrah, R. Silerova, *Phys. Chem. Chem. Phys.* **2002**, *4*, 3436-3442.
[27] A. Nitzan, M. A. Ratner, *Science* **2003**, *300*, 1384-1389.
[28] L. Cai, M. A. Cabassi, H. C. Yoon, O. M. Cabarcos, C. L. McGuiness, A. K. Flatt, D. L. Allara, J. M. Tour, T. S. Mayer, *Nano Lett.* **2005**, *5*, 2365-2372.
[29] P. A. Lewis, C. E. Inman, F. Maya, J. M. Tour, J. E. Hutchison, P. S. Weiss, *J. Am. Chem. Soc.* **2005**, *127*, 17421-17426.
[30] N. Weibel, S. Grunder, M. Mayor, *Org. Biomol. Chem.* **2007**, *5*, 2343-2353.
[31] A. Villares, S. Martin, I. Giner, J. Diaz, D. P. Lydon, P. Low, P. Cea, *Soft Matter* **2008**, *4*, 1508-1514.
[32] L. M. Ballesteros, S. Martín, G. Pera, P. A. Schauer, N. J. Kay, M. C. López, P. J. Low, R. J. Nichols, P. Cea, *Langmuir* **2011**, *27*, 3600-3610.
[33] L. M. Ballesteros, S. Martín, C. Momblona, S. Marqués-González, M. C. López, R. J. Nichols, P. J. Low, P. Cea, *J. Phys. Chem. C.* **2012**, *116*, 9142-9150.
[34] T. Baunach, V. Ivanova, D. M. Kolb, H. G. Boyen, P. Ziemann, M. Buttner, P. Oelhafen, *Adv. Mater.* **2004**, *16*, 2024-2028.
[35] H. G. Boyen, P. Ziemann, U. Wiedwald, V. Ivanova, D. M. Kolb, S. Sakong, A. Gross, A. Romanyuk, M. Buttner, P. Oelhafen, *Nat. Mater.* **2006**, *5*, 394-399.
[36] M. Manolova, V. Ivanova, D. M. Kolb, H. G. Boyen, P. Ziemann, M. Buttner, A. Romanyuk, P. Oelhafen, *Surf. Sci.* **2005**, *590*, 146-153.
[37] C. Silien, D. Lahaye, M. Caffio, R. Schaub, N. R. Champness, M. Buck, *Langmuir* **2011**, *27*, 2567-2574.

[38] R. E. Martin, F. Diederich, *Angew. Chem. Int. Ed.* **1999**, *38*, 1350-1377.
[39] S. Creager, C. J. Yu, C. Bamdad, S. O'Connor, T. MacLean, E. Lam, Y. Chong, G. T. Olsen, J. Luo, M. Gozin, J. F. Kayyem, *J. Am. Chem. Soc.* **1999**, *121*, 1059-1064.
[40] X. Cui, A. Primak, Z. Zarate, J. Tomfohr, O. F. Sankey, A. J. Moore, T. A. Moore, D. Gust, G. Harris, S. M. Lindsay, *Science* **2001**, *294*, 571-574.
[41] U. H. F. Bunz, *Acc. Chem. Res.* **2001**, *34*, 988-1010.
[42] Z. J. Donhauser, B. A. Mantooth, K. F. Kelly, L. A. Bumm, J. D. Monnell, J. J. Stapleton, D. W. Price Jr, A. M. Rawlett, D. L. Allara, J. M. Tour, P. S. Weiss, *Science* **2001**, *292*, 2303-2307.
[43] X. Xiao, L. A. Nagahara, A. M. Rawlett, N. Tao, *J. Am. Chem. Soc.* **2005**, *127*, 9235-9240.
[44] R. Huber, M. T. Gonzalez, S. Wu, M. Langer, S. Grunder, V. Horhoiu, M. Mayor, M. R. Bryce, C. S. Wang, R. Jitchati, C. Schonenberger, M. Calame, *J. Am. Chem. Soc.* **2008**, *130*, 1080-1084.
[45] S. Wu, M. T. Gonzalez, R. Huber, S. Grunder, M. Mayor, C. Schonenberger, M. Calame, *Nat. Nanotechnol.* **2008**, *9*, 569-574.
[46] A. M. Moore, B. A. Mantooth, Z. Donhauser, Y. Yao, J. M. Tour, P. S. Weiss, *J. Am. Chem. Soc.* **2007**, *129*, 10352.
[47] G. Pera, S. Martín, L. M. Ballesteros, A. J. Hope, P. J. Low, R. J. Nichols, P. Cea, *Chem. Eur. J.* **2010**, *16*, 13398-13405.
[48] S. Martin, I. Grace, M. R. Bryce, C. S. Wang, R. Jitchati, A. S. Batsanov, S. Higgins, C. J. Lambert, R. J. Nichols, *J. Am. Chem. Soc.* **2010**, *132*, 9157-9164.
[49] W. Hong, H. Li, S.-X. Liu, Y. Fu, J. Li, V. Kaliginedi, S. Decurtins, T. Wandlowski, *J. Am. Chem. Soc.* **2012**, *134*, 19425-19431.
[50] C. M. Guédon, H. Valkenier, T. Markussen, K. S. Thygesen, J. C. Hummelen, J. v. d. Molen, *Nat. Nanotechnol.* **2012**, *7*, 304-308.
[51] C. R. Parker, Z. Wei, C. R. Arroyo, K. Jennum, T. Li, M. Santella, N. Bovet, G. Shao, H. Wenping, H. S. J. Van der Zant, M. Vanin, G. C. Solomon, B. W. Laursen, K. Norgaard, M. B. Nielsen, *Adv. Mater.* **2013**, *25*, 405-409.
[52] S. Marqués-González, D. S. Yufit, J. A. K. Howard, S. Martin, H. M. Osorio, V. M. Garcia-Suarez, R. J. Nichols, S. J. Higgins, P. Cea, P. J. Low, *Dalton Trans.* **2013**, *42*, 338-341.
[53] N. Katsonis, A. Marchenko, S. Taillemite, D. Fichou, G. Chouraqui, C. Aubert, M. M., *Chem. Eur. J.* **2003**, *9*, 2574-2581.
[54] N. Katsonis, A. Marchenko, D. Fichou, N. Barret, *Surf. Sci.* **2008**, *602*, 9-16.
[55] A. Beeby, K. Findlay, P. J. Low, T. B. Marder, *J. Am. Chem. Soc.* **2002**, *124*, 8280-8284.
[56] W. Haiss, N. T. K. Thanh, J. Aveyard, D. G. Ferning, *Anal. Chem.* **2007**, *79*, 4215-4221.
[57] H. G. Boyen, G. Kästle, F. Weigl, B. Koslowski, C. Dietrich, P. Ziemann, J. P. Spatz, S. Riethmüller, C. Hartmann, M. Möller, G. Schmid, M. G. Garnier, P. Oelhafen, *Science* **2002**, *297*, 1533-1536.
[58] C. Shan, H. Yang, D. Han, Q. Zhang, A. Ivaska, L. Niu, *Biosens Bioelectron* **2010**, *25*, 1070-1074.
[59] G. Liu, E. Luais, J. J. Gooding, *Langmuir* **2011**, *27*, 4176-4183.
[60] Y.-Y. Fong, B. R. Visser, J. R. Gascooke, B. C. C. Cowie, L. Thomsen, G. F. Metha, M. A. Buntine, H. H. Harris, *Langmuir* **2011**, *27*, 8099-8104.
[61] K. Kurihara, J. Kiling, P. Stenius, J. H. Fendler, *J. Am. Chem. Soc.* **1983**, *105*, 2574-2579.

[62] Y. Yonezawa, T. Sato, M. Ohno, H. Hada, *J. Chem. Soc., Faraday Trans I* **1987**, *83*, 1559-1567.
[63] A. C. Dürr, F. Schreiber, M. Kelsch, H. D. Carstanjen, H. Dosch, *Adv. Mater.* **2002**, *14*, 961-963.
[64] A. V. Walker, T. B. Tighe, J. Stapleton, B. C. Haynie, S. Upilli, D. L. Allara, N. Winograd, *Appl. Phys. Lett.* **2004**, *84*, 4008-4010.
[65] C. Silien, M. Buck, *J. Phys. Chem. C* **2008**, *112*, 3881-3890.
[66] B. Pittenger, N. Erina, D. Su, *Application Note Veeco Instruments Inc*, **2010**.
[67] T. J. Young, M. A. Monglus, T. L. Burnett, W. R. Broughton, S. L. Ogin, P. A. Smith, *Meas Sci. Technol* **2011**, *22*, 125703.
[68] K. Sweers, K. van der Werf, M. Bennink, V. Bubramaniam, *Nanoscale Res. Lett.* **2011**, *6*, 270.
[69] G. Lee, H. Lee, K. Nam, J.-H. Han, J. Yang, S. W. Lee, D. S. Yoon, K. Eom, T. Kwon, *Nanoscale Res. Lett.* **2012**, *7*, 608.
[70] W. Haiss, D. Lackey, J. K. Sass, *J. Chem. Phys.* **1991**, *95*, 2193-2196.

TOC